Prenatal methamphetamine exposure is associated with corticostriatal white matter changes in neonates

Fleur L Warton[1], **Paul A Taylor**[1,2,3,4], **Christopher MR Warton**[1], **Christopher D Molteno**[5], **Pia Wintermark**[6], **Nadine M Lindinger**[1,7], **Lilla Zöllei**[8], **Andre van der Kouwe**[8], **Joseph L Jacobson**[1,5,9], **Sandra W Jacobson**[1,5,9], and **Ernesta M Meintjes**[1,2]

[1]Department of Human Biology, Faculty of Health Sciences, University of Cape Town, South Africa

[2]MRC/UCT Medical Imaging Research Unit, Division of Biomedical Engineering, Faculty of Health Sciences, University of Cape Town, South Africa

[3]African Institute for Mathematical Sciences, South Africa

[4]Scientific and Statistical Computing Core, National Institutes of Health, Bethesda, Maryland, USA

[5]Department of Psychiatry and Mental Health, Faculty of Health Sciences, University of Cape Town, South Africa

[6]Department of Pediatrics, McGill University, Montreal Children's Hospital, Montreal, Canada

[7]ACSENT Laboratory, Department of Psychology, University of Cape Town, South Africa

[8]Athinoula A. Martinos Centre for Biomedical Imaging, Massachusetts General Hospital, Charlestown, MA, USA

[9]Department of Psychiatry and Behavioral Neurosciences, Wayne State University School of Medicine, Detroit, MI, USA

Abstract

Diffusion tensor imaging (DTI) studies have shown that prenatal exposure to methamphetamine is associated with alterations in white matter microstructure, but to date no tractography studies have been performed in neonates. The striato-thalamo-orbitofrontal circuit and its associated limbic-striatal areas, the primary circuit responsible for reinforcement, has been postulated to be

Address correspondence to: Fleur L. Warton: fleur.warton@gmail.com; +27 72 979 8729.

dysfunctional in drug addiction. This study investigated potential white matter changes in the striatal-orbitofrontal circuit in neonates with prenatal methamphetamine exposure. Mothers were recruited antenatally and interviewed regarding methamphetamine use during pregnancy, and DTI sequences were acquired in the first postnatal month. Target regions of interest were manually delineated, white matter bundles connecting pairs of targets were determined using probabilistic tractography in AFNI-FATCAT, and fractional anisotrophy (FA) and diffusion measures were determined in white matter connections. Regression analysis showed that increasing methamphetamine exposure was associated with reduced FA in several connections between the striatum and midbrain, orbital frontal cortex, and associated limbic structures, following adjustment for potential confounding variables. Our results are consistent with previous findings in older children and extend them to show that these changes are already evident in neonates. The observed alterations are likely to play a role in the deficits in attention and inhibitory control frequently seen in children with prenatal methamphetamine exposure.

Keywords

Magnetic resonance imaging; diffusion tensor imaging; prenatal methamphetamine exposure; neonate; corticostriatal white matter

INTRODUCTION

The abuse of methamphetamine is one of the most rapidly growing drug problems worldwide, (Panenka et al. 2013), with particularly high prevalence in East and South-east Asia and Oceania (UNODC 2017a). Studies suggest that it is second only to marijuana in global use (Courtney and Ray 2014; UNODC 2017b). The rate of methamphetamine dependence among adult women in southern sub-Saharan Africa is equivalent to the global rate (0.18%) (Degenhardt et al. 2014). Within the Cape Coloured community of the Western Cape, the rate of methamphetamine ("tik") abuse is the highest in South Africa (Peltzer et al. 2010); 35–43% of patients seeking treatment for drug abuse report it as their primary drug (Meade et al. 2015). Methamphetamine is a potent psychostimulant, exerting its effects primarily on the central nervous system (CNS) by altering the release and activity of the monoaminergic neurotransmitters, dopamine, norepinephrine and serotonin (Riddle et al. 2006). Although the mechanisms of action of methamphetamine are not fully understood, a large body of preclinical and clinical literature has demonstrated its neurotoxicity. Structural and metabolic alterations in a number of brain areas, including the basal ganglia (Chang et al. 2005), hippocampus (Thompson et al. 2004), amygdala (Orikabe et al. 2011), thalamus (Volkow et al. 2001) and a range of cortical regions (London et al. 2005), have been observed in both current and abstinent users, and several studies have shown an association between methamphetamine-induced neurostructural damage and altered cognitive or affective function (Thompson et al. 2004; Tanabe et al. 2009).

A multi-site study in the United States estimated the incidence of methamphetamine use by pregnant women at over 5% (Arria et al. 2006). In the Cape Flats region of the Western Cape, South Africa, a recent study found that 8.1% of pregnant women had used methamphetamine within the last three months (Petersen Williams et al. 2014).

Methamphetamine causes vasoconstriction and reduced placental blood flow (Stek et al. 1995). It is associated with increased placental weight and surface area, a possible consequence of chronic hypoxia (Carter et al. 2016), a condition that has been observed in the methamphetamine-exposed fetus (LaGasse et al. 2011). A range of adverse perinatal effects on both mother and infant have been associated with methamphetamine use in pregnancy, including higher incidence of gestational hypertension and preeclampsia and increased risk of fetal and neonatal death (Gorman et al. 2014). Gestational age at birth has been observed to be lower in exposed infants (Nguyen et al. 2010), with an increased risk of preterm birth (Ladhani et al. 2011). Methamphetamine exposure has also been shown to be associated with smaller size at birth (Nguyen et al. 2010; Ladhani et al. 2011), and lower birth weight (Ladhani et al. 2011).

In the light of the above-mentioned effects and the well-documented neurotoxicity of methamphetamine in adult abusers, it is reasonable to hypothesize that exposure during the neurologically vulnerable prenatal period might induce potentially severe and long-term neurostructural alterations. CNS growth and development is rapid and complex during gestation (Dubois et al. 2014), and the influence of a highly neuroactive drug such as methamphetamine might well be expected to induce significant structural modifications.

Diffusion tensor imaging (DTI) is a neuroimaging modality that enables visualisation and characterisation of white matter within the CNS by analysing the three-dimensional diffusion of water molecules within fibre bundles (Feldman et al. 2010). From the extracted data several measures of the structural integrity of the white matter bundles and their component axons can be determined. Axial diffusivity (AD) is a measure of the diffusion of water molecules in the direction parallel to the white matter fibres, while radial diffusivity (RD) measures perpendicular movement. The most widely used measure of water movement is fractional anisotropy (FA), which represents the normalised variance of the total diffusivities (Assaf and Pasternak 2008). Higher FA indicates diffusion that is primarily in a direction parallel to the longitudinal axis of the white matter fibre bundles (Feldman et al. 2010) and is generally regarded as a marker of more healthy, highly structured or mature white matter (Alexander et al. 2007).

Information from DT images relating to the directionality and alignment of water diffusion can be used by tractography algorithms to estimate the locations of white matter (WM) fibre bundles within the brain (Assaf and Pasternak 2008). Tractography is often performed by defining one or more target regions of interest (ROIs), among which the most likely locations of WM connections (WMCs) are calculated; then, the average properties of the connections can be compared statistically both at the network and per-connection level. Diffusion measures within a fibre bundle have been shown to indicate functional impairment in pathologies that affect the microstructure and organisation of CNS white matter, such as multiple sclerosis, Alzheimer's disease and temporal lobe epilepsy(Alexander et al. 2007), and DTI is a valuable tool for investigating and quantifying the extent and nature of these effects.

An appreciable body of evidence shows significant effects of methamphetamine use on diffusion measures. Recently abstinent methamphetamine users exhibit reduced FA in

frontal cortical regions (Alicata et al. 2009; Tobias et al. 2010) and in the genu of the corpus callosum (CC) (Kim et al. 2009; Tobias et al. 2010), and higher AD and RD have been noted in the caudate and putamen of methamphetamine users (Alicata et al. 2009).

In the light of these findings, it is reasonable to hypothesise that prenatal methamphetamine exposure might exert similar deleterious effects on CNS structure in the exposed fetus. There is a sparsity of DT imaging literature examining such effects, however, and the results to date are inconsistent. Lower FA and increased AD and RD were observed in white matter tracts passing through striatal, limbic and frontal cortical regions of 6- to 7-year-old children with prenatal methamphetamine exposure (Roos et al. 2015). An investigation of infants with combined methamphetamine/tobacco exposure demonstrated reduced FA in superior, anterior and posterior corona radiata, with increased diffusivity in these regions (Chang et al. 2016). In a study of 9- to 11-year-old children, however, prenatal exposure was associated with higher FA in the genu of the CC, corona radiata and internal and external capsules (Colby et al. 2012), and similar results were observed in a voxel-based study of a 3- to 4-year-old cohort, which noted increased FA and reduced diffusivity in genu and splenium of the CC, frontal and parietal white matter and the basal ganglia (Cloak et al. 2009).

There is thus agreement in the literature that *in utero* exposure to methamphetamine induces significant and enduring effects on CNS white matter, but the precise nature of these changes is not clear. Moreover, to date there are no published studies of DT tractography in neonates with prenatal methamphetamine exposure. Children born to women who abuse methamphetamine are almost invariably exposed to a suboptimal postnatal rearing environment (Nguyen et al. 2010), which is likely to have strong effects on neural development. Investigations of neonatal cohorts permit a cleaner separation of substance exposure effects from the potential confounding influences of the postnatal environment.

The orbitofrontal cortex (OFC) plays a fundamental role in stimulus-reinforcement and reversal learning and thus in modulating motivational, emotional and social behaviour (Rolls 2004), and is essential in the processes underlying inhibitory control and goal-directed behaviour (Cole et al. 2012). It projects primarily to the ventral striatum, which consists of the nucleus accumbens, ventral putamen and ventromedial caudate nucleus (Haber et al. 1995), as well as to the head and body of the caudate (Haber et al. 1995) and convergence zones within the caudate and putamen in the dorsal striatum (Jarbo and Verstynen 2015). The ventral striatum also receives input from the hippocampus and areas associated with the limbic regions, such as the amygdala and ventral tegmental area in the midbrain (Nakano 2000). As the primary circuit responsible for reinforcement, the striato-thalamo-orbitofrontal circuit, with its associated limbic-striatal areas, has been postulated to be dysfunctional in drug addiction and to mediate the compulsive drug-seeking behaviour noted in addicted subjects (Volkow and Fowler 2000).

A considerable body of evidence demonstrates alterations in components of this system following prenatal exposure to methamphetamine. Mice exposed to methamphetamine *in utero* showed significantly increased impulsivity, reduced inhibitory control and heightened motivation for reward (Lloyd et al. 2013), behavioural characteristics which mimic core symptoms of addiction in humans and may indicate dysfunction in the striato-frontal cortex

circuits. Similarly, children with prenatal methamphetamine exposure have been shown to have reduced caudate, putamen and hippocampal volumes (Chang et al. 2004) as well as reduced volume of the pars opercularis (Roos et al. 2014), a frontal cortical region which is associated with inhibitory control (Aron et al. 2004). Methamphetamine-exposed children exhibit altered metabolism in the striatum (Smith et al. 2001) and lower activation in the OFC and putamen during the performance of a working memory task (Roussotte et al. 2011).

In a previous whole-brain network-based analysis of a cohort of South African children with and without prenatal methamphetamine exposure, we found altered diffusivity and reduced FA in the three major classes of white matter tracts (commissural, projection and association fibres), indicating a generalised effect of methamphetamine exposure on white matter microstructure (Warton et al. 2017). The current study was designed to extend these findings by examining white matter fibre bundles forming part of the corticostriatal and mesolimbic connections between OFC and subcortical regions of interest (ROIs) which had previously been manually defined in this cohort. It was hypothesised that prenatal methamphetamine exposure would be associated with microstructural alterations within these connections.

METHODS

Study sample

The sample consisted of infants born to women from the Cape Coloured (mixed ancestry) community from Cape Town, South Africa, where there is a very high prevalence of methamphetamine use among disadvantaged pregnant women (Petersen Williams et al. 2014). They were selected from a larger prospective longitudinal study of prenatal alcohol and drug exposure on infant development (Taylor et al. 2015; Carter et al. 2016; Jacobson et al. 2017). The exposed group was comprised of infants with prenatal exposure to methamphetamine, while the control group consisted of infants from the same community without methamphetamine exposure and with minimal or no exposure to alcohol or other drugs of abuse *in utero*.

Pregnant women were recruited following antenatal care bookings at two midwife obstetric care units in the community. They were interviewed three times during pregnancy with regard to their use of methamphetamine and other drugs (days/month) and cigarette smoking (cigarettes/day). Alcohol consumption was determined using time-line follow-back interviews (Jacobson et al. 2002, 2017). The current sample consisted of women who reported use of methamphetamine on at least 2 occasions per month during pregnancy. The control group included women who did not use illicit drugs other than marijuana. All but one control abstained from alcohol use during pregnancy; one control drank only 1–2 drinks on 2 occasions during the pregnancy).

Informed consent was obtained from each mother at recruitment and at the laboratory and neuroimaging visits. Approval for the study was obtained from the ethics committees at Wayne State University and the Faculty of Health Sciences of the University of Cape Town.

Scanning

Newborns were scanned without use of sedation following procedures developed by PW, SJ, and colleagues (Jacobson et al. 2017) (mean age at scan = 2.7 wk, range = 1–5 wk postpartum, with the exception of one infant, born at 31 wk gestational age, who was scanned at 9 wk of age). Scanning took place at the Cape Universities Brain Imaging Centre (CUBIC).

The infants were brought to CUBIC a minimum of 1 hour prior to scanning. During the pre-scan period the infants were weighed, head circumference and crown-to-heel length were measured, and a neonatal behavioral assessment was conducted by CM (Brazelton 1984). The infant was then firmly swaddled and placed in a VacFix® vacuum cushion (S&S Par Scientific, Houston, TX) following an adapted protocol for neuroimaging of nonsedated neonates (Laswad et al. 2009). Earplugs were used to protect the infant from scanner noise. The infant was fed by the mother and allowed to fall asleep. A pulse and oxygen saturation monitor probe was secured to the infant's foot, and this was monitored during the scanning process by a developmental paediatrician, or by a research nurse, who remained in the scanner room with the infant throughout the procedure.

MRI scanning was performed using a Siemens 3T Allegra scanner. A circularly polarised bird-cage coil, custom-built for use with neonates, was used for transmission and reception of the signal. Two diffusion weighted imaging (DWI) sets with opposite (AP/PA) phase encoding directions were acquired with a twice refocused spin echo EPI sequence. For 5 infants (1 with methamphetamine exposure, 4 controls), the scanning parameters were as follows: TR 9500 ms, TE 86 ms, matrix 50 slices of 80×80 voxels, voxel size $2\times2\times2$ mm^3. The remaining infants were scanned using a similar DTI sequence which also included navigation for performing real-time motion detection and correction (Alhamud et al. 2012), using the same scanning parameters as above, but with TR = 10 026 ms. In both navigated and non-navigated sequences, AP and PA acquisitions each contained four $b = 0$ s mm^{-2} reference scans and 30 DW gradient directions with $b = 1000$ s mm^{-2}.

For anatomical imaging, a motion-navigated multiecho gradient echo sequence (van der Kouwe et al. 2008) was used, with protocol parameters as follows: FOV 114 mm, 128 slices of 144×144 voxels, voxel size $1\times1\times1$ mm^3, TR 20 ms, TE 1.46/ 3.14/ 4.82/ 6.5/ 8.18/ 9.86/11.54/ 13.22 ms. Two sets were acquired, with flip angles of 5° and 20°, respectively.

Data processing and parameter estimation

DWI data were inspected visually for motion artifacts and dropout slices, and individual poor quality volumes were discarded. At least 12 DWIs remained for each infant; there was no difference between exposed and control groups in number of remaining DWIs ($p = 0.815$). Any scan which did not meet this threshold was excluded from further analysis. Motion and EPI distortion were corrected using FSL's eddy correct and topup tools (Smith et al. 2004). DTs and tensor parameters such as FA, eigenvalues (L_i, i=1,2,3; AD=L_1; RD=$[L_2+L_3]/2$) and directional eigenvectors ($\mathbf{e}_i$, i=1,2,3) were estimated using AFNI (Cox 1996).

For the anatomical images, individual echoes from the two flip angle acquisitions were combined using mri_ms_fitparms using FreeSurfer (Fischl et al. 2004). From this, tissue parameters were estimated and a single image volume, with an optimal contrast flip angle of 24°, was synthesised.

Manual tracing of target regions of interest

Regions of interest were viewed and manually delineated using Freeview software (the FreeSurfer image analysis suite http://surfer.nmr.mgh.harvard.edu/; version 5.0) run on a Lenovo ThinkPad X220 tablet (see Fig. 1). The following ROIs were used bilaterally as targets for tractographic analysis: OFC, caudate, nucleus accumbens, putamen, hippocampus, and amygdala. The midbrain was also traced, as a single structure in the midline.

Caudate nucleus and nucleus accumbens (NAcc)—An oblique line from the inferior tip of the lateral ventricle to the midpoint of the inferior boundary of the internal capsule was drawn to separate the caudate and nucleus accumbens, while a line descending from the middle of the inferior border of the anterior limb of the internal capsule was taken to define the boundary between the putamen and the nucleus accumbens. Posteriorly, the caudate diminishes in size and eventually becomes difficult to define as the tail reaches the point where it curves inferiorly posterior to the thalamus. For this reason the posterior and inferior portions of the caudate were not traced.

Putamen—Tracing of the putamen was done in the axial or coronal planes on a slice by slice basis, as the junction of putamen and pallidum was generally most clearly seen in axial sections.

Hippocampus—The hippocampus was traced primarily in the coronal plane, with considerable guidance from views in the sagittal plane. It can be seen in sagittal sections within the temporal lobe as a sausage-shaped structure. More anteriorly in the coronal plane the hippocampal head appears, and the structure becomes large and rounded.

Amygdala—The amygdala is located anterior to the head of the hippocampus. It is bounded in its anterior, inferior and lateral aspects by white matter, and postero-inferiorly by the hippocampus and the tip of the lateral ventricle. The tracings of the amygdala were done in all three planes, as it was difficult to see in its entirety in any one plane.

Midbrain—The region described as midbrain included the complete midbrain (as defined anatomically), encompassing tectum, tegmentum, and crus cerebri. The lower border corresponded with the mesencephalic/pontine boundary at the upper border of the basilar pons. Superiorly, care was taken to exclude the subthalamic area which is easily identifiable in neonatal brains.

Orbitofrontal cortex—The OFC was defined as that area of cortex situated on the inferior surface of the frontal lobe. Its anterior and lateral borders were defined by the hemispheric edge where the lateral and inferior frontal surfaces meet. Its posterior boundary was defined by the posterior edge of cortex on the inferior surface. The OFC was traced in one control

subject, following which nonlinear registration was performed between the $b0$ reference volume of this subject and each of the others in the study using AFNI's 3dQwarp. The calculated transformation was then applied to map the ROIs into each subject's native diffusion space.

Tractographic analysis

Probabilistic tractography was performed using the FATCAT software in AFNI (Taylor and Saad 2013). Local uncertainties in DT eigenvectors and FA were estimated with FATCAT, and probabilistic tractography was performed using 3dTrackID, which uses repeated iterations of whole brain tracking with the FACTID algorithm (Taylor et al. 2012) to estimate the most likely locations of white matter connections between pairs of targets. The tract propagation parameters were as follows: maximum "turning" angle of 55°, through voxels with FA > 0.1, which is the standard threshold for FA as a proxy for white matter in infants (Dubois et al. 2006). 5000 iterations of whole brain tracking were performed, and all voxels through which more than 500 tracts passed to connect a pair of targets were included to create white matter connections (WMCs) associated with each pair of targets. The mean and standard deviation of the DTI parameters FA, AD and RD for each WMC were automatically calculated by the FATCAT tracking function. Only WMCs found between the same pairs of targets in all subjects were included for further analysis, in order to compare properties of similar locations of the WM skeleton.

Statistical analysis

Statistics were performed using IBM SPSS Statistics (version 23; IBM, Armonk, NY). Acquisition sequence (navigated or non-navigated) was included as a confounding variable in all models. Additionally, 10 control variables were examined as potential confounders: maternal alcohol use (in units of absolute alcohol consumed per day across pregnancy), marijuana use (days per month during pregnancy), and cigarette smoking during pregnancy (number of cigarettes per day during pregnancy); maternal education (number of years completed), marital status (married/unmarried), parity, and socioeconomic status (Hollingshead 2011) (SES); and infant sex, gestational age at scan (in weeks), and birth weight (grams).

All variables were examined for normality of distribution, and outliers more than 3 standard deviations from the mean were transformed by recoding to one unit greater than the next highest value (Winer 1971); this transformation was applied to the methamphetamine, alcohol, marijuana and cigarette smoking exposure measures. Sample characteristics were compared between exposed and control groups using t-tests for continuous variables and chi-square tests for categorical variables. Sample characteristics were also compared between subjects whose scans were included in the tractographic analyses and those whose scans were discarded owing to poor quality or excessive motion.

Analysis of covariance (ANCOVA) was used to compare mean FA within each WMC between exposed and control groups, adjusting for acquisition sequence. Control variables associated with the FA ($p < 0.05$) within each WMC were added in a second ANCOVA to adjust for potential confounders. For WMCs in which group differences in FA were

significant, differences in mean values of AD and RD were examined using the same procedure. AD and RD were also analysed within the WMCs in which FA differences fell short of significance ($0.10 > p > 0.05$) as exploratory analyses to reduce the risk of Type 2 error given the small sample size.

Regression analyses were used to investigate potential associations between a continuous measure of methamphetamine exposure (number of days/month of pregnancy that methamphetamine was used by the mother) and structural WM properties (e.g., mean FA in each WMC), adjusting for acquisition sequence. WMCs in which FA was significantly related to prenatal methamphetamine exposure and those where the association fell just short of significance ($p < 0.10$) were then examined further by means of hierarchical multiple regression with best estimate approach. Confounding variables related to FA ($p < 0.05$) were entered individually (starting with the most strongly related to FA in the tract of interest and proceeding to the weakest). Variables which altered the standardized regression coefficient for methamphetamine by less than 10% at step of entry were omitted from the final model. WMCs in which a significant or trend-level ($p < 0.10$) association between FA and methamphetamine exposure was observed were further analysed in hierarchical regression analyses in relation to AD and RD.

RESULTS

Sample characteristics

The study sample consisted of 23 infants, 11 (5 male) with methamphetamine exposure and 12 (7 male) non-exposed controls. The demographic characteristics of the sample are summarised in Table 1. Of the maternal background characteristics, only maternal education was significantly different between groups, with mothers in the methamphetamine group having completed about 1 year less education than those in the control group.

In comparing substance use, there were no significant alcohol or drug between-group differences except (as planned) for methamphetamine. Mean cigarette use by the mothers of the exposed group was somewhat higher than that of the control group.

17 additional subjects were scanned but did not achieve an acceptable scan quality owing to excessive motion during the scan or high levels of motion artifact during initial or later processing, and were thus not included in the tractographic analysis. Sample characteristics were compared between infants whose scans were analysed and those whose scans were discarded (see Table 2). There were no between group differences for any demographic or substance exposure variables.

Tractographic connections

Probabilistic tractography yielded 31 WMCs between target ROIs that were common to all infants. These are defined by the pair of target ROIs connected by each WMC and are shown in Table 3, along with the mean and standard deviation of FA, AD and RD for each region. For visualisation purposes, Figure 2 displays a set of mini-probabilistic fibre tracts generated between the pairs of traced ROIs in one control infant brain (Taylor et al. 2015).

Comparison of mean WMC parameters between the methamphetamine and control groups

The comparisons of mean FA in WMCs of methamphetamine exposed and control infants are shown in Table 4. Regions showing at least trend-level significance ($p < 0.10$) are shown, with significant associations ($p < 0.05$) highlighted. With the inclusion of acquisition sequence as an obligatory control variable, mean FA was observed to be significantly lower ($p < 0.05$) in the methamphetamine group in 4 WMCs: midbrain – left putamen, left putamen – left OFC, right putamen – right OFC, and right putamen – right amygdala. After controlling for additional potential confounding variables (listed in Table 3), the FA reductions in the midbrain – left putamen, right putamen – right OFC, and right putamen – right amygdala remained significant.

To further investigate the structural changes, AD and RD values were compared between groups in the same regions showing FA differences. Table 5 shows the results of the comparison of mean RD in WMCs that showed significant or near significant differences in mean FA between groups. Increased RD in the methamphetamine group was observed in two WMCs (midbrain – right caudate and right putamen – right OFC). Following the addition of potential confounding variables, only increased RD in the midbrain – right caudate connection continued to be significant. No significant differences were observed in mean AD between methamphetamine exposed and control groups at any stage of the analysis in any WMC (all p's > 0.10).

Regression of tract parameters on methamphetamine exposure

To compare WM structural properties with the quantitative degree of exposure, mean FA values in each of the WMCs were linearly modelled in terms of the maternal methamphetamine use and relevant potential confounding variables. The results of the regression analyses are shown in Table 6. Linear regression including acquisition sequence as a confounding variable confirmed the group contrasts in all WMCs except the midbrain – left putamen connection and revealed significant associations of increasing methamphetamine exposure with reduced FA in 5 additional connections: midbrain – right caudate; midbrain – right putamen; left NAcc – left OFC; right NAcc – right OFC; midbrain – right hippocampus.

Potential confounding variables were included in subsequent regression analyses if they showed a correlation with FA in the relevant WMC at $p < 0.05$. After controlling for confounders, associations of increased methamphetamine exposure with FA reductions in 7 of the 8 WMCs survived.

The association of AD and RD with quantitative methamphetamine exposure was explored in each of the WMCs in which FA and exposure showed an association at $p < 0.10$. Linear regression including acquisition sequence as an obligatory control variable in all WMCs showed that increasing methamphetamine exposure was associated with increased RD in the left caudate – right caudate connection ($\beta = 0.531$, $p = 0.016$). After adjustment for potential confounders, this association between RD and methamphetamine remained significant, while two additional connections (midbrain – right caudate and midbrain – right putamen) fell short of significance (p's < 0.10). A trend for association between increasing

methamphetamine exposure and increased AD was observed in the left caudate – right caudate connection ($p < 0.10$) but no other associations between AD and methamphetamine exposure were observed in any connection at any stage of the analysis (all p's > 0.10).

DISCUSSION

This is the first study to use DTI tractography to examine the microstructural effects of prenatal methamphetamine exposure on white matter connections between defined brain regions in neonates. As hypothesised, methamphetamine exposure was shown to be associated with reduced FA in several WMCs involving striatal structures, the midbrain and the OFC. The right hemisphere appeared more strongly affected, with 7 right and 3 left hemisphere connections revealing methamphetamine-associated alterations in FA, notwithstanding that findings in neonates are generally "widespread," given that cognitive development and hemispheric dominance are as yet relatively unrefined. Effects of methamphetamine on other diffusion measures were less extensive. No significant effects were observed on AD - the maximum amount of DT-modelled diffusion in a voxel - alone. By contrast, RD (i.e. the average amount of diffusion perpendicular to the main axis in each voxel) was observed to be increased in association with methamphetamine exposure in a small subset of the connections showing reduced FA.

Several of these results observed in neonates are consistent with previous studies examining white matter alterations in older infants and children with prenatal methamphetamine exposure. In a study of children (aged 6–7 yr), methamphetamine exposure was associated with significantly reduced FA in the left external capsule and fornix, measured in the putamen, pallidum, hippocampus, amygdala and OFC regions (Roos et al. 2015). Similarly, infants (aged 0–4 months) with combined methamphetamine/tobacco exposure were observed to have reduced FA in superior, anterior and posterior corona radiata (Chang et al. 2016). Both of these studies also reported increased RD in the corresponding regions, in agreement with the findings of the current study. In the older cohort increased AD was also observed, although this was not found in the same regions which exhibited reduced FA (Roos et al. 2015). Additionally, a number of DTI studies of adult methamphetamine users reported structural changes similar to those observed in the current study, with reduced FA noted in frontal white matter (Alicata et al. 2009; Tobias et al. 2010) and CC (Kim et al. 2009; Tobias et al. 2010). While these populations have a different mode of exposure to methamphetamine (by direct usage rather than prenatally), it is interesting that similar WM effects are observed in both.

It should be noted, however, that two other studies of prenatal methamphetamine exposure reported WM changes that were contrary to those observed in the present study. Increased FA was observed in older children (9–11 yr) with prenatal exposure to methamphetamine and alcohol in a number of white matter tracts, including the anterior and posterior limbs of the internal capsule, anterior corona radiata and genu of the corpus callosum, in the left hemisphere (Colby et al. 2012). Similarly, reduced diffusivity was observed in frontal and parietal white matter in young children (3–4 yr) with prenatal methamphetamine exposure (Cloak et al. 2009). Variations in methodology may account for these discrepancies, such as the use of voxel-based analyses rather than a tractographic approach as used in the current

study. Additionally, no exposure data were reported for the study in which increased FA was observed (Colby et al. 2012), raising the possibility that the exposure levels were lower than in the current study. In support of this explanation is the observation that mean cumulative exposure in the study which observed reduced diffusivity (Cloak et al. 2009) was considerably lower than that in which increased FA was observed in neonates (Chang et al. 2016).

The relations between structural and functional alterations in the brain and diffusion indices are complex and remain uncertain. Anisotropic water diffusion in neural tissue is primarily a product of intact axonal membranes, with the presence and integrity of the myelin sheath playing a modulating role (Beaulieu 2002). FA is thus generally regarded as a measure of the structural coherence of the white matter under consideration (Taylor et al. 2015), with higher FA reflecting greater restriction of diffusion and presumably more highly organised structure (Feldman et al. 2010). FA reductions have been demonstrated in the white matter of subjects with neurodegenerative disorders, such as Alzheimer's disease (Duan et al. 2006) and in psychiatric conditions, such as schizophrenia (Tang et al. 2007). FA changes may be a consequence of altered myelin extent or structure (Mori and Zhang 2006), damage to the axon fibres (Assaf and Pasternak 2008) or changes in water content, such as in edema (Hüppi and Dubois 2006). Reduced FA may be the result of increased RD or reduced AD, or a combination of alterations in both measures (Mori and Zhang 2006; Alexander et al. 2007), and investigation of these indices can provide some elucidation as to the nature of the underlying pathology, as AD is generally more sensitive to axonal damage (Wu et al. 2007), while RD changes have been shown to reflect changes in myelination (Song et al. 2005).

As observed previously, *in utero* methamphetamine exposure was associated in the current study with reduced FA in a number of white matter connections. Investigation of the diffusion indices showed no changes in AD in any of the studied connections, and only a small subset of the regions with reduced FA exhibited increased RD in association with methamphetamine exposure. These findings indicate that exposure to methamphetamine reduced the integrity of the white matter in the studied neonates, and the changes in RD suggest that damage to or alterations in myelin may have played a role in this. In addition, *in vitro* methamphetamine treatment has been shown to induce apoptosis in oligodendroglial cells (Genc et al. 2003), and in animal studies prenatal exposure to methamphetamine has been associated with reduced myelination and myelin content of white matter (Melo et al. 2006). Given that RD changes were observed in only a small number of connections, however, these conclusions should be drawn with caution.

An additional consideration when interpreting diffusion data from infants, and one that adds considerable complexity, is that neural development is active and ongoing in neonates. Axonal organisation into fibre systems begins in the first trimester of pregnancy (Dubois et al. 2014), and at birth most of the major white matter tracts are in place (Ouyang et al. 2015). The process of myelination, however, is far from complete at birth (Dubois et al. 2006). In addition, white matter maturation is region specific: it appears to follow a caudal-to-rostral and central-to-peripheral progression, such that proximal pathways and central regions will be myelinated earlier and more rapidly than distal and polar ones (Dubois et al. 2014). Myelination also tends to occur earlier in functional systems used earlier in life than

those used later, so that sensory pathways and projection fibres mature sooner than motor and association connections (Dubois et al. 2006). Anisotropy has been shown to be present in white matter prior to myelination (Beaulieu 2002) and is measurable even during gestation (Mitter et al. 2015), but the rapid and anatomically non-uniform development of the white matter postnatally results in a natural shift in diffusion measures (Beaulieu 2002). A variety of factors may play a role in this, including increased fibre diameter and cohesion of tracts, myelination, reduced brain water and denser axonal packing (Mabbott et al. 2006). As the white matter tracts mature, FA tends to increase while AD and RD decrease (Qiu et al. 2015). Given that in the current study methamphetamine exposure was associated with reduced FA, there is the additional possibility that these changes may be an indication of slower maturation of neonatal white matter. Delayed maturation of serotonergic neurons in the frontal cortex (Tavares et al. 1996), and inhibited somatic and locomotor development (McDonnell-Dowling et al. 2014) have been observed in rats following treatment with methamphetamine *in utero*. This interpretation would be consistent with a previous study of infants with prenatal methamphetamine and tobacco exposure, which noted reduced FA and increased diffusivity in the corona radiata at 1 month, and demonstrated that the developmental trajectories of these indices were altered in comparison to healthy comparison infants (Chang et al. 2016). However, as studies have observed diffusion and anisotropy differences in white matter of older children with prenatal exposure, it is unlikely that the changes observed are solely an indication of a delay in white matter development.

The basal ganglia are involved in regulating much of the activity of the frontal cortex, including motor function and a range of cognitive and emotional behaviours (Bonelli and Cummings 2007). The OFC and its connections with the striatum and associated subcortical limbic regions are involved in motivation and reward (Rolls 2004), and alterations in these regions have been suggested to underlie some of the behavioural dysfunction observed in addiction (Volkow and Fowler 2000). The current findings of decreased FA in the orbitofrontal-striatal circuit and associated limbic and midbrain connections thus suggest that the damage induced by methamphetamine exposure is not limited to the cortex and subcortical grey matter structures but includes the white matter bundles connecting them. Damage to these circuits has significant functional implications. Microstructural damage to the orbitofrontal-striatal circuit has been demonstrated in individuals with a clinical diagnosis of attention deficit hyperactivity disorder (ADHD) (Wu et al. 2014; Gau et al. 2015) and reduced generalised FA in the orbitofrontal-striatal connection has been associated with increased inattention (Wu et al. 2014; Gau et al. 2015), impaired executive function and severity of clinical symptoms (Shang et al. 2013) in children with ADHD. Children with prenatal methamphetamine exposure have a significantly increased incidence of ADHD (Piper et al. 2011) and increased measures of ADHD clinical symptoms (Kiblawi et al. 2013). Prenatal methamphetamine exposure has also been associated with significantly poorer performance on tasks of sustained attention (Chang et al. 2004) and inhibitory control (Derauf et al. 2012) and increased risk of neurobehavioural disinhibition (Himes et al. 2014). A recent study of 6- to 7-year-old children with prenatal methamphetamine exposure showed significant impairments in a range of cognitive domains associated with executive function (Kwiatkowski et al. 2017). It is not unreasonable to speculate that alterations in the

corticostriatal circuits, such as those demonstrated in the current study, play a role in at least some of the cognitive deficits exhibited by methamphetamine-exposed children.

There are certain limitations inherent in studies of prenatal drug exposure which may be addressed by investigating effects during the neonatal period. One such weakness is the influence of postnatal environment. Children who are exposed to methamphetamine *in utero* are often born into a disadvantaged environment (Piper et al. 2011; Derauf et al. 2012), which has itself been shown to exert a damaging influence on behavioural and neurostructural development (Avants et al. 2015). The potentially strong confounding effects of the postnatal environment can, however, be controlled to a substantial degree by investigating exposure effects in neonates, as in the current study. An additional advantage of this study was the ascertainment of exposure parameters prospectively during pregnancy. The women whose infants were studied here were recruited during pregnancy, and methamphetamine and poly-substance use was assessed by maternal report on three occasions during pregnancy. This provides a significant advantage over retrospective studies of older children, in which accurate determination of maternal drug use during pregnancy is difficult, and permits a more accurate measure of frequency of methamphetamine use and a more informed quantitative analysis of its effects.

There are a number of limitations in the current study. The potential confounding effects of polysubstance exposure is almost inevitable in any study investigating prenatal drug effects (Sowell et al. 2010). This is a significant concern, as exposure to alcohol, marijuana and tobacco has been shown to be associated with altered structure and function of the CNS (Liu et al. 2011; Taylor et al. 2015). Some individuals in the control and methamphetamine-using groups in the current study reported drinking low levels of alcohol (median = 0 drinks/occasion) and smoking cigarettes (median = 4.3 cigarettes/day) and marijuana (median = 0 days/month). However, alcohol and marijuana use did not differ between groups. Although cigarette smoking was weakly related to methamphetamine use, it was not significantly different between groups, and the regression models adjusted for any potential confounding effects. Prenatal exposure to tobacco has been shown to increase FA in the frontal white matter (Jacobsen et al. 2007), and women using methamphetamine have been observed to smoke more cigarettes than women who smoke but do not use methamphetamine (Chang et al. 2016), so that the effect of cigarette smoking on infant white matter is likely to be compounded in the methamphetamine group. However, the accuracy of substance use recall permitted by prenatal recruitment and prospective interview during pregnancy enabled a quantitatively reliable measurement of these variables, and they were analysed as potential confounders and included where statistically relevant. The sample size was small, although comparable to that in a previous study (Roos et al. 2015). For this reason, a less stringent *p*-value (0.10) was used to determine which WMCs were examined in the exploratory analyses, although we have focused primarily on those connections in which FA reached conventional levels of statistical significance in the Discussion. In addition, the significance level was not adjusted for multiple comparisons. However, the number of significant effects on FA in the regression analyses (Table 5)—9 out of 31 WMCs (29.0%)—clearly exceeded the 5.0% expected by chance. Moreover, with a larger cohort more alterations might have reached significance.

This is the first study, to our knowledge, to use DTI tractography to investigate methamphetamine-associated microstructural alterations in corticostriatal and limbic connections in neonates. The previous literature is equivocal, but the current results agree with findings of reduced anisotropy and increased RD in white matter connections in association with prenatal methamphetamine exposure and extend them to show that these changes are measurable in infants in the first postnatal month. These alterations may well underlie a subset of the cognitive dysfunction exhibited by children with prenatal methamphetamine exposure. Further investigations are essential to determine the extent to which methamphetamine-induced white matter damage is associated with functional deficits.

Acknowledgments

References

Alexander AL, Lee JE, Lazar M, Field AS. Diffusion tensor imaging of the brain. Neurotherapeutics. 2007; 4:316–29. DOI: 10.1016/j.nurt.2007.05.011 [PubMed: 17599699]

Alhamud A, Tisdall MD, Hess AT, et al. Volumetric navigators for real-time motion correction in diffusion tensor imaging. Magn Reson Med. 2012; 68:1097–108. DOI: 10.1002/mrm.23314 [PubMed: 22246720]

Alicata D, Chang L, Cloak C, et al. Higher diffusion in striatum and lower fractional anisotropy in white matter of methamphetamine users. Psychiatry Res. 2009; 174:1–8. DOI: 10.1016/j.pscychresns.2009.03.011 [PubMed: 19782540]

Aron AR, Robbins TW, Poldrack RA. Inhibition and the right inferior frontal cortex. Trends Cogn Sci. 2004; 8:170–177. DOI: 10.1016/j.tics.2004.02.010 [PubMed: 15050513]

Arria AM, Derauf C, Lagasse LL, et al. Methamphetamine and other substance use during pregnancy: preliminary estimates from the Infant Development, Environment, and Lifestyle (IDEAL) study. Matern Child Health J. 2006; 10:293–302. DOI: 10.1007/s10995-005-0052-0 [PubMed: 16395620]

Assaf Y, Pasternak O. Diffusion tensor imaging (DTI)-based white matter mapping in brain research: a review. J Mol Neurosci. 2008; 34:51–61. DOI: 10.1007/s12031-007-0029-0 [PubMed: 18157658]

Avants BB, Hackman DA, Betancourt LM, et al. Relation of childhood home environment to cortical thickness in late adolescence: specificity of experience and timing. PLoS One. 2015; 10:e0138217.doi: 10.1371/journal.pone.0138217 [PubMed: 26509809]

Beaulieu C. The basis of anisotropic water diffusion in the nervous system - a technical review. NMR Biomed. 2002; 15:435–55. DOI: 10.1002/nbm.782 [PubMed: 12489094]

Bonelli RM, Cummings JL. Frontal-subcortical circuitry and behavior. Dialogues Clin Neurosci. 2007; 9:141–51. DOI: 10.1001/archneur.1993.00540080076020 [PubMed: 17726913]

Brazelton, TB. Neonatal behavioral assessment scale. 2nd. J.B. Lippincott Co; 1984.

Carter RC, Wainwright H, Molteno CD, et al. Alcohol, methamphetamine, and marijuana exposure have distinct effects on the human placenta. Alcohol Clin Exp Res. 2016; 40:753–64. DOI: 10.1111/acer.13022 [PubMed: 27038593]

Chang L, Cloak C, Patterson K, et al. Enlarged striatum in abstinent methamphetamine abusers: A possible compensatory response. Biol Psychiatry. 2005; 57:967–974. DOI: 10.1016/j.biopsych. 2005.01.039 [PubMed: 15860336]

Chang L, Oishi K, Skranes J, et al. Sex-specific alterations of white matter developmental trajectories in infants with prenatal exposure to methamphetamine and tobacco. JAMA psychiatry. 2016; 73:1217–1227. DOI: 10.1001/jamapsychiatry.2016.2794 [PubMed: 27829078]

Chang L, Smith LM, LoPresti C, et al. Smaller subcortical volumes and cognitive deficits in children with prenatal methamphetamine exposure. Psychiatry Res. 2004; 132:95–106. DOI: 10.1016/j.pscychresns.2004.06.004 [PubMed: 15598544]

Cloak CC, Ernst T, Fujii L, et al. Lower diffusion in white matter of children with prenatal methamphetamine exposure. Neurology. 2009; 72:2068–75. DOI: 10.1212/01.wnl. 0000346516.49126.20 [PubMed: 19369643]

Colby JB, Smith L, O'Connor MJ, et al. White matter microstructural alterations in children with prenatal methamphetamine/polydrug exposure. Psychiatry Res. 2012; 204:140–8. DOI: 10.1016/j.pscychresns.2012.04.017 [PubMed: 23149028]

Cole DM, Beckmann CF, Searle GE, et al. Orbitofrontal connectivity with resting-state networks is associated with midbrain dopamine D3 receptor availability. Cereb Cortex. 2012; 22:2784–2793. DOI: 10.1093/cercor/bhr354 [PubMed: 22186675]

Courtney KE, Ray LA. Methamphetamine: An update on epidemiology, pharmacology, clinical phenomenology, and treatment literature. Drug Alcohol Depend. 2014; 143:11–21. DOI: 10.1016/j.drugalcdep.2014.08.003 [PubMed: 25176528]

Cox RW. AFNI: software for analysis and visualization of functional magnetic resonance neuroimages. Comput Biomed Res. 1996; 29:162–73. DOI: 10.1006/cbmr.1996.0014 [PubMed: 8812068]

Degenhardt L, Baxter AJ, Lee YY, et al. The global epidemiology and burden of psychostimulant dependence: Findings from the Global Burden of Disease Study 2010. Drug Alcohol Depend. 2014; 137:36–47. DOI: 10.1016/j.drugalcdep.2013.12.025 [PubMed: 24559607]

Derauf C, Lagasse LL, Smith LM, et al. Prenatal methamphetamine exposure and inhibitory control among young school-age children. J Pediatr. 2012; 161:452–9. DOI: 10.1016/j.jpeds.2012.02.002 [PubMed: 22424953]

Duan J-H, Wang H-Q, Xu J, et al. White matter damage of patients with Alzheimer's disease correlated with the decreased cognitive function. Surg Radiol Anat. 2006; 28:150–156. DOI: 10.1007/s00276-006-0111-2 [PubMed: 16614789]

Dubois J, Dehaene-Lambertz G, Kulikova S, et al. The early development of brain white matter: A review of imaging studies in fetuses, newborns and infants. Neuroscience. 2014; 276:48–71. DOI: 10.1016/j.neuroscience.2013.12.044 [PubMed: 24378955]

Dubois J, Hertz-Pannier L, Dehaene-Lambertz G, et al. Assessment of the early organization and maturation of infants' cerebral white matter fiber bundles: a feasibility study using quantitative diffusion tensor imaging and tractography. Neuroimage. 2006; 30:1121–32. DOI: 10.1016/j.neuroimage.2005.11.022 [PubMed: 16413790]

Feldman HM, Yeatman JD, Lee ES, et al. Diffusion tensor imaging: a review for pediatric researchers and clinicians. J Dev Behav Pediatr. 2010; 31:346–56. DOI: 10.1097/DBP.0b013e3181dcaa8b [PubMed: 20453582]

Fischl B, Salat DH, van der Kouwe AJW, et al. Sequence-independent segmentation of magnetic resonance images. Neuroimage. 2004; 23(Suppl 1):S69–84. DOI: 10.1016/j.neuroimage. 2004.07.016 [PubMed: 15501102]

Gau SS, Tseng W-L, Tseng W-YI, et al. Association between microstructural integrity of frontostriatal tracts and school functioning: ADHD symptoms and executive function as mediators. Psychol Med. 2015; 45:529–43. DOI: 10.1017/S0033291714001664 [PubMed: 25075643]

Genc K, Genc S, Kizildag S, et al. Methamphetamine induces oligodendroglial cell death in vitro. Brain Res. 2003; 982:125–30. DOI: 10.1016/S0006-8993(03)02890-7 [PubMed: 12915247]

Gorman MC, Orme KS, Nguyen NT, et al. Outcomes in pregnancies complicated by methamphetamine use. Am J Obstet Gynecol. 2014; 211:429.e1–7. DOI: 10.1016/j.ajog. 2014.06.005 [PubMed: 24905417]

Haber SN, Kunishio K, Mizobuchi M, Lynd-Balta E. The orbital and medial prefrontal circuit through the primate basal ganglia. J Neurosci. 1995; 15:4851–67. [PubMed: 7623116]

Himes SK, LaGasse LL, Derauf C, et al. Risk of neurobehavioral disinhibition in prenatal methamphetamine-exposed young children with positive hair toxicology results. Ther Drug Monit. 2014; 36:535–43. DOI: 10.1097/FTD.0000000000000049 [PubMed: 24518561]

Hollingshead AB. Four factor index of social status. Yale J Sociol. 2011; 8:21–52.

Hüppi PS, Dubois J. Diffusion tensor imaging of brain development. Semin Fetal Neonatal Med. 2006; 11:489–97. DOI: 10.1016/j.siny.2006.07.006 [PubMed: 16962837]

Jacobsen LK, Picciotto MR, Heath CJ, et al. Prenatal and adolescent exposure to tobacco smoke modulates the development of white matter microstructure. J Neurosci. 2007; 27:13491–8. DOI: 10.1523/JNEUROSCI.2402-07.2007 [PubMed: 18057207]

Jacobson SW, Chiodo LM, Sokol RJ, Jacobson JL. Validity of maternal report of prenatal alcohol, cocaine, and smoking in relation to neurobehavioral outcome. Pediatrics. 2002; 109:815–25. DOI: 10.1542/peds.109.5.815 [PubMed: 11986441]

Jacobson SW, Jacobson JL, Molteno CD, et al. Heavy prenatal alcohol exposure is related to smaller corpus callosum in newborn MRI scans. Alcohol Clin Exp Res. 2017; 41:965–975. DOI: 10.1111/acer.13363 [PubMed: 28247416]

Jarbo K, Verstynen TD. Converging structural and functional connectivity of orbitofrontal, dorsolateral prefrontal, and posterior parietal cortex in the human striatum. J Neurosci. 2015; 35:3865–78. DOI: 10.1523/JNEUROSCI.2636-14.2015 [PubMed: 25740516]

Kiblawi ZN, Smith LM, LaGasse LL, et al. The effect of prenatal methamphetamine exposure on attention as assessed by continuous performance tests: results from the Infant Development, Environment, and Lifestyle study. J Dev Behav Pediatr. 2013; 34:31–7. DOI: 10.1097/DBP. 0b013e318277a1c5 [PubMed: 23275056]

Kim I-S, Kim Y-T, Song H-J, et al. Reduced corpus callosum white matter microstructural integrity revealed by diffusion tensor eigenvalues in abstinent methamphetamine addicts. Neurotoxicology. 2009; 30:209–13. DOI: 10.1016/j.neuro.2008.12.002 [PubMed: 19135475]

Kwiatkowski MA, Donald KA, Stein DJ, et al. Cognitive outcomes in prenatal methamphetamine exposed children aged six to seven years. Compr Psychiatry. 2017; doi: 10.1016/j.comppsych. 2017.08.003

Ladhani NNN, Shah PS, Murphy KE, Knowledge Synthesis Group on Determinants of Preterm/LBW Births. Prenatal amphetamine exposure and birth outcomes: a systematic review and metaanalysis. Am J Obstet Gynecol. 2011; 205:219.e1–7. DOI: 10.1016/j.ajog.2011.04.016 [PubMed: 21658669]

LaGasse LL, Wouldes T, Newman E, et al. Prenatal methamphetamine exposure and neonatal neurobehavioral outcome in the USA and New Zealand. Neurotoxicol Teratol. 2011; 33:166–75. DOI: 10.1016/j.ntt.2010.06.009 [PubMed: 20615464]

Laswad T, Wintermark P, Alamo L, et al. Method for performing cerebral perfusion-weighted MRI in neonates. Pediatr Radiol. 2009; 39:260–4. DOI: 10.1007/s00247-008-1081-9 [PubMed: 19104796]

Liu J, Cohen RA, Gongvatana A, et al. Impact of prenatal exposure to cocaine and tobacco on diffusion tensor imaging and sensation seeking in adolescents. J Pediatr. 2011; 159:771–5. DOI: 10.1016/j.jpeds.2011.05.020 [PubMed: 21723565]

Lloyd SA, Oltean C, Pass H, et al. Prenatal exposure to psychostimulants increases impulsivity, compulsivity, and motivation for rewards in adult mice. Physiol Behav. 2013; 119:43–51. DOI: 10.1016/j.physbeh.2013.05.038 [PubMed: 23739493]

London ED, Berman SM, Voytek B, et al. Cerebral metabolic dysfunction and impaired vigilance in recently abstinent methamphetamine abusers. Biol Psychiatry. 2005; 58:770–8. DOI: 10.1016/j.biopsych.2005.04.039 [PubMed: 16095568]

Mabbott DJ, Noseworthy M, Bouffet E, et al. White matter growth as a mechanism of cognitive development in children. Neuroimage. 2006; 33:936–46. DOI: 10.1016/j.neuroimage.2006.07.024 [PubMed: 16978884]

McDonnell-Dowling K, Donlon M, Kelly JP. Methamphetamine exposure during pregnancy at pharmacological doses produces neurodevelopmental and behavioural effects in rat offspring. Int J Dev Neurosci. 2014; 35:42–51. DOI: 10.1016/j.ijdevneu.2014.03.005 [PubMed: 24667147]

Meade CS, Towe SL, Watt MH, et al. Addiction and treatment experiences among active methamphetamine users recruited from a township community in Cape Town, South Africa: A mixed-methods study. Drug Alcohol Depend. 2015; 152:79–86. DOI: 10.1016/j.drugalcdep. 2015.04.016 [PubMed: 25977205]

Melo P, Moreno VZ, Vázquez SP, et al. Myelination changes in the rat optic nerve after prenatal exposure to methamphetamine. Brain Res. 2006; 1106:21–9. DOI: 10.1016/j.brainres.2006.05.020 [PubMed: 16842764]

Mitter C, Prayer D, Brugger PC, et al. In vivo tractography of fetal association fibers. PLoS One. 2015; 10:e0119536.doi: 10.1371/journal.pone.0119536 [PubMed: 25742520]

Mori S, Zhang J. Principles of diffusion tensor imaging and its applications to basic neuroscience research. Neuron. 2006; 51:527–39. DOI: 10.1016/j.neuron.2006.08.012 [PubMed: 16950152]

Nakano K. Neural circuits and topographic organization of the basal ganglia and related regions. Brain Dev. 2000; 22(Suppl 1):S5–16. [PubMed: 10984656]

Nguyen D, Smith LM, Lagasse LL, et al. Intrauterine growth of infants exposed to prenatal methamphetamine: results from the infant development, environment, and lifestyle study. J Pediatr. 2010; 157:337–9. DOI: 10.1016/j.jpeds.2010.04.024 [PubMed: 20570284]

Orikabe L, Yamasue H, Inoue H, et al. Reduced amygdala and hippocampal volumes in patients with methamphetamine psychosis. Schizophr Res. 2011; 132:183–9. DOI: 10.1016/j.schres. 2011.07.006 [PubMed: 21784619]

Ouyang A, Jeon T, Sunkin SM, et al. Spatial mapping of structural and connectional imaging data for the developing human brain with diffusion tensor imaging. Methods. 2015; 73:27–37. DOI: 10.1016/j.ymeth.2014.10.025 [PubMed: 25448302]

Panenka WJ, Procyshyn RM, Lecomte T, et al. Methamphetamine use: a comprehensive review of molecular, preclinical and clinical findings. Drug Alcohol Depend. 2013; 129:167–79. DOI: 10.1016/j.drugalcdep.2012.11.016 [PubMed: 23273775]

Peltzer K, Ramlagan S, Johnson BD, Phaswana-Mafuya N. Illicit drug use and treatment in South Africa: a review. Subst Use Misuse. 2010; 45:2221–43. DOI: 10.3109/10826084.2010.481594 [PubMed: 21039113]

Petersen Williams P, Jordaan E, Mathews C, et al. Alcohol and Other Drug Use during Pregnancy among Women Attending Midwife Obstetric Units in the Cape Metropole, South Africa. Adv Prev Med. 2014; 2014:871427.doi: 10.1155/2014/871427 [PubMed: 24639899]

Piper BJ, Acevedo SF, Kolchugina GK, et al. Abnormalities in parentally rated executive function in methamphetamine/polysubstance exposed children. Pharmacol Biochem Behav. 2011; 98:432–9. DOI: 10.1016/j.pbb.2011.02.013 [PubMed: 21334365]

Qiu A, Mori S, Miller MI. Diffusion tensor imaging for understanding brain development in early life. Annu Rev Psychol. 2015; 66:853–76. DOI: 10.1146/annurev-psych-010814-015340 [PubMed: 25559117]

Riddle EL, Fleckenstein AE, Hanson GR. Mechanisms of methamphetamine-induced dopaminergic neurotoxicity. AAPS J. 2006; 8:E413–8. [PubMed: 16808044]

Rolls ET. The functions of the orbitofrontal cortex. Brain Cogn. 2004; 55:11–29. DOI: 10.1016/ S0278-2626(03)00277-X [PubMed: 15134840]

Roos A, Jones G, Howells FM, et al. Structural brain changes in prenatal methamphetamine-exposed children. Metab Brain Dis. 2014; 29:341–9. DOI: 10.1007/s11011-014-9500-0 [PubMed: 24553878]

Roos A, Kwiatkowski MA, Fouche J, et al. White matter integrity and cognitive performance in children with prenatal methamphetamine exposure. Behav Brain Res. 2015; 279:62–7. DOI: 10.1016/j.bbr.2014.11.005 [PubMed: 25446763]

Roussotte FF, Bramen JE, Nunez SC, et al. Abnormal brain activation during working memory in children with prenatal exposure to drugs of abuse: the effects of methamphetamine, alcohol, and polydrug exposure. Neuroimage. 2011; 54:3067–75. DOI: 10.1016/j.neuroimage.2010.10.072 [PubMed: 21040792]

Saad ZS, Reynolds RC. SUMA. Neuroimage. 2012; 62:768–73. DOI: 10.1016/j.neuroimage. 2011.09.016 [PubMed: 21945692]

Shang CY, Wu YH, Gau SS, Tseng WY. Disturbed microstructural integrity of the frontostriatal fiber pathways and executive dysfunction in children with attention deficit hyperactivity disorder. Psychol Med. 2013; 43:1093–107. DOI: 10.1017/S0033291712001869 [PubMed: 22894768]

Smith LM, Chang L, Yonekura ML, et al. Brain proton magnetic resonance spectroscopy in children exposed to methamphetamine in utero. Neurology. 2001; 57:255–60. DOI: 10.1212/WNL.57.2.255 [PubMed: 11468309]

Smith SM, Jenkinson M, Woolrich MW, et al. Advances in functional and structural MR image analysis and implementation as FSL. Neuroimage. 2004; 23(Suppl 1):S208–19. DOI: 10.1016/j.neuroimage.2004.07.051 [PubMed: 15501092]

Song S, Yoshino J, Le TQ, et al. Demyelination increases radial diffusivity in corpus callosum of mouse brain. Neuroimage. 2005; 26:132–40. DOI: 10.1016/j.neuroimage.2005.01.028 [PubMed: 15862213]

Sowell ER, Leow AD, Bookheimer SY, et al. Differentiating prenatal exposure to methamphetamine and alcohol versus alcohol and not methamphetamine using tensor-based brain morphometry and discriminant analysis. J Neurosci. 2010; 30:3876–85. DOI: 10.1523/JNEUROSCI.4967-09.2010 [PubMed: 20237258]

Stek AM, Baker RS, Fisher BK, et al. Fetal responses to maternal and fetal methamphetamine administration in sheep. Am J Obstet Gynecol. 1995; 173:1592–8. [PubMed: 7503206]

Tanabe J, Tregellas JR, Dalwani M, et al. Medial orbitofrontal cortex gray matter is reduced in abstinent substance-dependent individuals. Biol Psychiatry. 2009; 65:160–4. DOI: 10.1016/j.biopsych.2008.07.030 [PubMed: 18801475]

Tang CY, Friedman J, Shungu D, et al. Correlations between Diffusion Tensor Imaging (DTI) and Magnetic Resonance Spectroscopy (1H MRS) in schizophrenic patients and normal controls. BMC Psychiatry. 2007; 7:25.doi: 10.1186/1471-244X-7-25 [PubMed: 17578565]

Tavares MA, Silva MC, Silva-Araújo A, et al. Effects of prenatal exposure to amphetamine in the medial prefrontal cortex of the rat. Int J Dev Neurosci. 1996; 14:585–96. [PubMed: 8930690]

Taylor PA, Cho K, Lin C, Biswal BB. Improving DTI tractography by including diagonal tract propagation. PLoS One. 2012; 7:e43415.doi: 10.1371/journal.pone.0043415 [PubMed: 22970125]

Taylor PA, Jacobson SW, van der Kouwe A, et al. A DTI-based tractography study of effects on brain structure associated with prenatal alcohol exposure in newborns. Hum Brain Mapp. 2015; 36:170–86. DOI: 10.1002/hbm.22620 [PubMed: 25182535]

Taylor PA, Saad ZS. FATCAT: (an efficient) Functional and Tractographic Connectivity Analysis Toolbox. Brain Connect. 2013; 3:523–35. DOI: 10.1089/brain.2013.0154 [PubMed: 23980912]

Thompson PM, Hayashi KM, Simon SL, et al. Structural abnormalities in the brains of human subjects who use methamphetamine. J Neurosci. 2004; 24:6028–36. DOI: 10.1523/JNEUROSCI. 0713-04.2004 [PubMed: 15229250]

Tobias MC, O'Neill J, Hudkins M, et al. White-matter abnormalities in brain during early abstinence from methamphetamine abuse. Psychopharmacology (Berl). 2010; 209:13–24. DOI: 10.1007/s00213-009-1761-7 [PubMed: 20101394]

UNODC. Market analysis of synthetic drugs. United Nations Office on Drugs and Crime; 2017a. World Drug Report 2017.

UNODC. Global overview of drug demand and supply. United Nations Office on Drugs and Crime; 2017b. World Drug Report 2017.

van der Kouwe AJW, Benner T, Salat DH, Fischl B. Brain morphometry with multiecho MPRAGE. Neuroimage. 2008; 40:559–69. DOI: 10.1016/j.neuroimage.2007.12.025 [PubMed: 18242102]

Volkow ND, Chang L, Wang GJ, et al. Higher cortical and lower subcortical metabolism in detoxified methamphetamine abusers. Am J Psychiatry. 2001; 158:383–9. DOI: 10.1176/appi.ajp.158.3.383 [PubMed: 11229978]

Volkow ND, Fowler JS. Addiction, a disease of compulsion and drive: involvement of the orbitofrontal cortex. Cereb Cortex. 2000; 10:318–25. DOI: 10.1093/cercor/10.3.318 [PubMed: 10731226]

Warton F, Taylor P, Warton C, et al. White matter microstructural alterations in neonates with prenatal exposure to methamphetamine. 23rd Annual Meeting of the Organization for Human Brain Mapping. 2017

Winer, B. Statistical principles in experimental design. 2nd. McGraw-Hill; 1971.

Wu Q, Butzkueven H, Gresle M, et al. MR diffusion changes correlate with ultra-structurally defined axonal degeneration in murine optic nerve. Neuroimage. 2007; 37:1138–47. DOI: 10.1016/j.neuroimage.2007.06.029 [PubMed: 17689104]

Wu Y-H, Gau SS-F, Lo Y-C, Tseng W-YI. White matter tract integrity of frontostriatal circuit in attention deficit hyperactivity disorder: association with attention performance and symptoms. Hum Brain Mapp. 2014; 35:199–212. DOI: 10.1002/hbm.22169 [PubMed: 22936578]
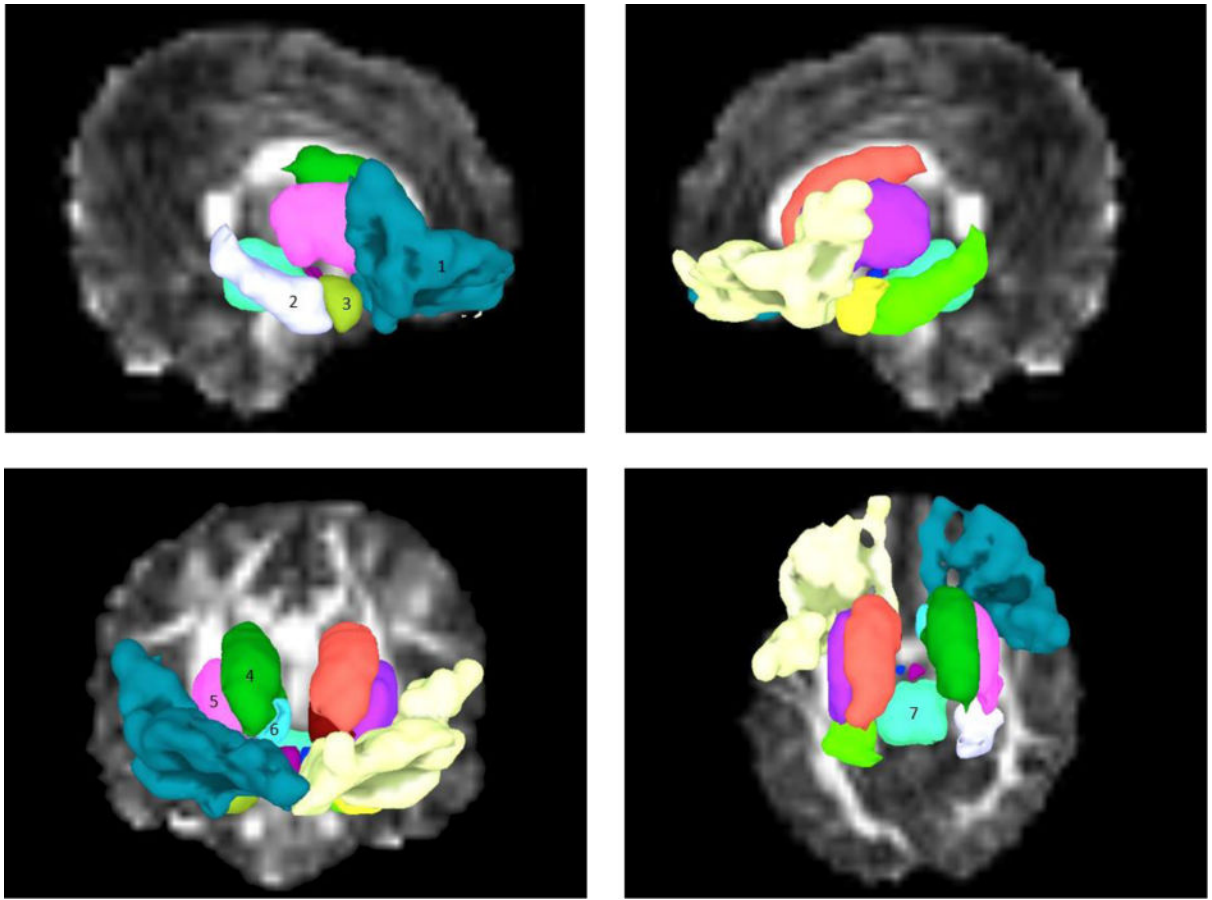
Fig. 1.
Traced ROIs used as targets for probabilistic tractography, shown in sagittal view in upper panels, and coronal and axial views in left and right lower panels respectively in SUMA (Saad and Reynolds 2012). 1) orbitofrontal cortex; 2) hippocampus; 3) amygdala; 4) caudate nucleus; 5) putamen; 6) nucleus accumbens; 7) midbrain. Regions are numbered in one hemisphere only but were traced bilaterally
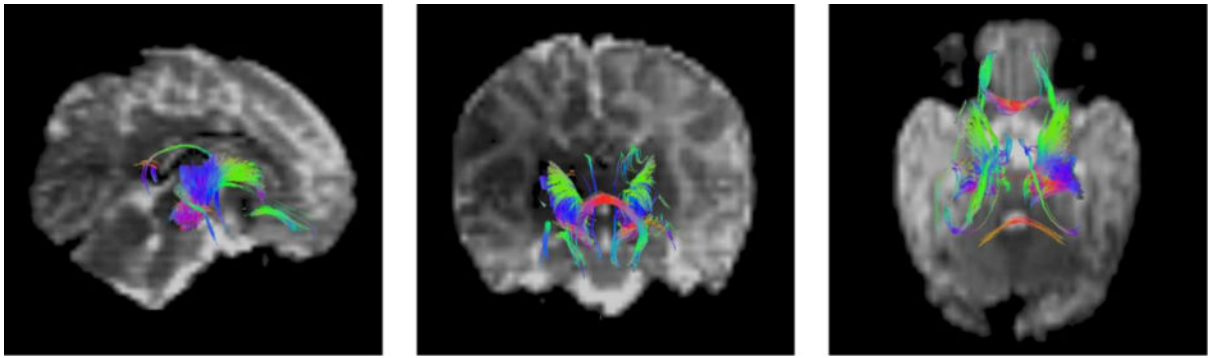
Fig. 2.
An example of representative white matter connection (WMC) structure generated using mini-probabilistic tractography connecting manually traced seed ROIs in one control infant brain. Full probabilistic tracking was used to calculate the WMCs used for statistical analysis. Colouration is by local tract direction, with left-right depicted in red, anterior-posterior in green, and inferior-superior in blue

Table 1

Sample characteristics (*N*=23).

	Methamphetamine (PEM) (*n*=11)			Control (Ctl) (*n* = 12)			χ^2 or *t*	*p*
	Mean	**SD**	**Range**	**Mean**	**SD**	**Range**		
Maternal								
Age (years)	27.2	3.9	21.4 – 32.6	25.1	5.4	18.8 – 36.4	-1.05	0.305
Education (years)	9.4	1.2	7.0 – 11.0	10.6	1.1	9.0 – 12.0	2.56	0.018
Parity	3.1	1.6	1 – 6	2.3	1.2	1 – 4	-1.44	0.165
Infant								
Sex (% male)	45.5			58.3			0.38	0.537
Birth weight (g)	2806.8	600.5	1370.0 – 3590.0	2795.8	485.2	1940.0 – 3470.0	-0.05	0.962
Gestational age at birth (weeks)	37.3	3.0	31.0 – 40.7	39.0	1.7	36.6 – 42.1	1.67	0.110
Gestational age at scan (weeks)	40.6	2.1	37.3 – 43.1	41.6	1.9	37.6 – 44.1	1.24	0.227
Substance use[a]								
Methamphetamine (days/month)	7.1	3.5	1.5 – 12.0	0.0	0.0	0.0 – 0.0	-7.04	0.000
Smoking (number cigarettes/day)	6.5[b]	5.4	2.0 – 20.0	3.3[c]	2.8	0.0 – 7.7	-1.78	0.089
Marijuana (days/month)	4.4[d]	9.6	0.0 – 30.5	0.0[e]	0.1	0.0 – 0.2	-1.58	0.129
Alcohol (oz AA/day)	0.2[f]	0.4	0.0 – 1.4	0.0[g]	0.0	0.0 – 0.1	-1.26	0.222

[a] mean, SD, range based on whole group (PEM, n=11; Ctl, n=12);

[b] 11/11 (100%) and

[c] 8/12 (66.7%) smoked cigarettes;

[d] 5/11 (45.5%) and

[e] 2/12 (16.7%) used marijuana;

[f] 5/11 (45.5%) and

[g] 1/12 (8.3%) drank alcohol during pregnancy.

Table 2

Comparison of scanned infants whose data were included vs. not included in the analyses (*N*=40).

	Included (n= 23)			Not included (n = 17)[a]			χ² or t	p
	Mean	SD	Range	Mean	SD	Range		
Maternal								
Age (years)	26.1	4.8	18.8 – 36.4	26.6	6.2	18.3 – 36.4	0.28	0.782
Education (years)	10.0	1.3	7.0 – 12.0	9.6	1.8	7.0 – 12.0	−0.86	0.398
Parity	2.7	1.4	1 – 6	3.1	1.8	1 – 6	0.80	0.429
Infant								
Sex (% male)	52.2			35.3			1.13	0.289
Birth weight (g)	2801.1	530.7	1370.0–3590.0	2873.8	418.6	2090.0–3490.0	0.47	0.643
Gestational age at birth (weeks)	38.2	2.5	31.0 – 42.1	38.7	2.3	33.7 – 42.1	0.71	0.485
Gestational age at scan (weeks)	41.1	2.0	37.3 – 44.1	41.0	2.0	36.7 – 44.6	−0.25	0.804
Substance use[a]								
Methamphetamine (days/month)	3.4[b]	4.3	0.0 – 12.0	1.7[c]	3.4	0.0 – 10.0	−1.28	0.208
Smoking (number cigarettes/day)	4.8[d]	4.5	0.0 – 20.0	5.7[e]	4.6	0.0 – 16.7	0.62	0.539
Marijuana (days/month)	2.1[f]	6.9	0.0 – 30.5	2.8[g]	5.3	0.0 – 17.7	0.33	0.746
Alcohol (oz AA/day)	0.1[h]	0.3	0.0 – 1.4	0.2[i]	0.3	0.0 – 1.0	1.16	0.253

[a] Infants who were scanned but whose scans were discarded: 5/17 (29.4%) too much motion during the scan, 7/17(41.1%) too many motion artifacts upon initial visual inspection, 5/17 (29.4%) too many artifacts upon later processing; Mean, SD, range based on whole group (Included, *n*=23; Not included, *n*=17);

[b] 11/23(48%) and

[c] 6/17 (35.3%) used methamphetamine;

[d] 19/23 (83%) and

[e] 14/17 (82.4%) smoked cigarettes;

[f] 6/23 (26%) and

[g] 5/17 (29.4%) used marijuana;

[h] 6/23 (26%) and

^{i}7/17 (41.1%) drank alcohol during pregnancy.

Table 3

White matter connections (WMCs) derived from probabilistic tractography across all subjects and the structural properties of each.

WMC	Methamphetamine (n=11) FA mean	SD	AD (×10⁻³ s/mm²) mean	SD	RD (×10⁻³ s/mm²) mean	SD	Control (n=12) FA mean	SD	AD (×10⁻³ s/mm²) mean	SD	RD (×10⁻³ s/mm²) mean	SD
Midbrain - Left Hippocampus	0.223	0.031	1.699	0.068	1.211	0.068	0.220	0.036	1.683	0.124	1.208	0.118
Midbrain - Right Hippocampus	0.227	0.027	1.682	0.084	1.190	0.077	0.232	0.028	1.705	0.079	1.195	0.066
Midbrain - Left Caudate	0.235	0.014	1.486	0.075	1.029	0.043	0.240	0.018	1.440	0.060	0.988	0.056
Midbrain - Right Caudate	0.230	0.014	1.469	0.069	1.028	0.039	0.248	0.044	1.455	0.061	0.986	0.068
Midbrain - Left Putamen	0.243	0.018	1.466	0.044	1.002	0.045	0.258	0.025	1.472	0.076	0.982	0.067
Midbrain - Right Putamen	0.245	0.012	1.467	0.050	1.002	0.035	0.252	0.020	1.440	0.034	0.970	0.046
Left OFC - Left NAcc	0.160	0.020	1.618	0.122	1.275	0.100	0.165	0.016	1.555	0.120	1.217	0.098
Right OFC - Right NAcc	0.161	0.019	1.622	0.107	1.273	0.090	0.167	0.028	1.583	0.099	1.232	0.104
Left OFC - Left Amygdala	0.176	0.024	1.813	0.196	1.396	0.177	0.184	0.028	1.773	0.135	1.346	0.128
Right OFC - Right Amygdala	0.178	0.029	1.780	0.159	1.366	0.161	0.179	0.032	1.827	0.180	1.398	0.165
Left OFC - Left Caudate	0.191	0.013	1.689	0.084	1.263	0.074	0.192	0.017	1.640	0.090	1.231	0.091
Right OFC - Right Caudate	0.189	0.017	1.703	0.067	1.278	0.073	0.199	0.031	1.683	0.096	1.243	0.108
Left OFC - Left Putamen	0.181	0.013	1.605	0.054	1.229	0.050	0.191	0.013	1.588	0.070	1.196	0.061
Right OFC - Right Putamen	0.176	0.011	1.632	0.078	1.258	0.071	0.190	0.019	1.593	0.081	1.199	0.077
Left OFC - Left Hippocampus	0.232	0.021	1.762	0.113	1.238	0.070	0.239	0.020	1.801	0.151	1.252	0.120
Left OFC - Right OFC	0.197	0.015	1.755	0.105	1.298	0.093	0.203	0.022	1.694	0.127	1.240	0.094
Right OFC - Left Caudate	0.221	0.022	1.771	0.083	1.256	0.082	0.249	0.084	1.749	0.131	1.179	0.138
Left Caudate - Left NAcc	0.176	0.018	1.722	0.134	1.319	0.094	0.175	0.022	1.642	0.111	1.261	0.096
Right Caudate - Right NAcc	0.182	0.018	1.734	0.116	1.316	0.074	0.184	0.027	1.692	0.132	1.283	0.105
Left Caudate - Left Putamen	0.199	0.015	1.542	0.046	1.136	0.041	0.202	0.014	1.496	0.064	1.098	0.062
Right Caudate - Right Putamen	0.201	0.015	1.545	0.056	1.135	0.044	0.203	0.016	1.520	0.072	1.113	0.064
Left Caudate - Right Caudate	0.284	0.019	1.875	0.115	1.201	0.092	0.290	0.025	1.816	0.108	1.150	0.082
Left Caudate - Left Hippocampus	0.241	0.017	1.678	0.122	1.159	0.091	0.253	0.022	1.709	0.144	1.156	0.114
Left Putamen - Left NAcc	0.169	0.013	1.454	0.069	1.127	0.059	0.175	0.019	1.404	0.057	1.076	0.046
Right Putamen - Right NAcc	0.168	0.022	1.458	0.068	1.131	0.049	0.175	0.021	1.442	0.064	1.108	0.059

WMC	Methamphetamine (n=11)						Control (n=12)					
	FA		AD ($\times 10^{-3}$ s/mm^2)		RD ($\times 10^{-3}$ s/mm^2)		FA		AD ($\times 10^{-3}$ s/mm^2)		RD ($\times 10^{-3}$ s/mm^2)	
	mean	SD	mean	SD	mean	SD	mean	SD	mean	SD	mean	SD
Left Hippocampus - Left Amygdala	0.198	0.023	1.564	0.070	1.151	0.054	0.197	0.025	1.567	0.074	1.156	0.083
Right Hippocampus - Right Amygdala	0.186	0.016	1.558	0.054	1.171	0.046	0.193	0.022	1.599	0.077	1.188	0.075
Left Putamen - Left Hippocampus	0.253	0.012	1.612	0.062	1.089	0.046	0.256	0.024	1.643	0.109	1.106	0.085
Right Putamen - Right Hippocampus	0.255	0.015	1.607	0.049	1.084	0.032	0.270	0.024	1.640	0.072	1.078	0.078
Left Putamen - Left Amygdala	0.220	0.030	1.478	0.063	1.052	0.081	0.242	0.027	1.499	0.053	1.029	0.078
Right Putamen - Right Amygdala	0.220	0.031	1.507	0.046	1.074	0.068	0.253	0.020	1.518	0.054	1.023	0.057

White matter connections are defined by target pairs. NAcc = nucleus accumbens; OFC = orbitofrontal cortex

Table 4

Group differences in FA in white matter connections (WMCs).

WMC	Methamphetamine (n=11)		Control (n=12)		F_{acq}	p_{acq}	F_{conf}	p_{conf}	Potential confounders
	Mean	SD	Mean	SD					
Midbrain - Right Caudate	0.230	0.014	0.248	0.044	3.33	0.083	3.33	0.083	none
Midbrain - Right Putamen	0.245	0.012	0.252	0.020	3.49	0.077	3.49	0.077	none
Midbrain - Left Putamen	0.243	0.018	0.258	0.025	**4.39**	**0.049**	**4.39**	**0.049**	none
Left Putamen - Left OFC	0.181	0.013	0.191	0.013	**5.65**	**0.028**	4.15	0.056	age
Right Putamen - Right OFC	0.176	0.011	0.190	0.019	**6.02**	**0.023**	**4.38**	**0.050**	age
Right Putamen - Right Amygdala	0.220	0.031	0.253	0.020	**7.48**	**0.013**	**7.48**	**0.013**	none
Right Putamen - Right Hippocampus	0.255	0.015	0.270	0.024	3.95	0.061	3.95	0.061	none

White matter connections are defined by target pairs. OFC = orbitofrontal cortex. Results with at least trend-level significance ($p < 010$) are displayed. F_{acq} = value controlling for acquisition sequence in the analysis; F_{conf}= value controlling for acquisition sequence and relevant potential confounding variables; significant effects ($p<0.05$) are highlighted in boldface. Age = gestational age at scan (weeks).

Table 5

Group differences in RD in white matter connections (WMCs) exhibiting FA differences (N=23).

WMC	Methamphetamine (n=11)		Control (n=12)		F_{acq}	p_{acq}	F_{conf}	p_{conf}	Confounders used
	Mean	SD	Mean	SD					
Midbrain - Right Caudate	1.028	0.039	0.986	0.068	**5.261**	**0.033**	**5.261**	**0.033**	none
Midbrain - Right Putamen	1.002	0.035	0.970	0.046	3.735	0.068	3.735	0.068	none
Right Putamen - Right OFC	1.258	0.071	1.199	0.077	**4.456**	**0.048**	2.988	0.100	age
Right Putamen - Right Amygdala	1.074	0.068	1.023	0.057	3.225	0.088	3.225	0.088	none

White matter connections are defined by target pairs. OFC = orbitofrontal cortex. Results with at least trend-level significance ($p < 010$) are displayed. F_{acq} = value when controlling for acquisition sequence in the analysis; F_{conf}= value following addition of acquisition sequence and significant confounding variables into analysis. Significant results (p<0.05) are highlighted in boldface. Age = gestational age at scan (weeks).

Table 6

Regression of FA in white matter connections (WMCs) with methamphetamine exposure ($N=23$).

WMC	β_{acq}	P_{acq}	β_{conf}	P_{conf}	Confounders included
Midbrain - Right Caudate	**-0.45**	**0.038**	**-0.45**	**0.038**	none
Midbrain - Right Putamen	**-0.41**	**0.048**	**-0.41**	**0.048**	none
Midbrain - Left Caudate	-0.38	0.089	-0.23	0.274	age
Midbrain - Left Putamen	-0.42	0.061	-0.42	0.061	none
Left NAcc - Left OFC	**-0.51**	**0.009**	**-0.44**	**0.020**	marital status
Left Putamen - Left OFC	**-0.57**	**0.007**	**-0.42**	**0.027**	age
Right NAcc - Right OFC	**-0.50**	**0.010**	**-0.50**	**0.010**	none
Right Caudate - Right OFC	-0.41	0.061	-0.25	0.211	age
Right Putamen - Right OFC	**-0.49**	**0.029**	**-0.364**	**0.094**	age
Midbrain - Right Hippocampus	**-0.49**	**0.018**	**-0.49**	**0.018**	none
Right Putamen - Right Amygdala	**-0.47**	**0.035**	**-0.47**	**0.035**	none
Right Putamen - Right Hippocampus	-0.43	0.060	-0.43	0.060	none
Left Caudate - Right Caudate	-0.41	0.060	-0.41	0.060	none
Left Caudate - Left Hippocampus	-0.44	0.054	-0.44	0.054	none
Left Hippocampus - Left OFC	-0.43	0.054	-0.43	0.054	none

White matter connections are defined by target pairs. NAcc = nucleus accumbens; OFC = orbitofrontal cortex. Results with at least trend-level significance ($p < 010$) are displayed. β_{acq} = value controlling for acquisition sequence in the analysis; β_{conf}= value following addition of acquisition sequence and significant confounding variables into analysis. Significant effects ($p<0.05$) are highlighted in boldface. Age = gestational age at scan (weeks).